



ALMA MATER STUDIORUM
UNIVERSITÀ DI BOLOGNA

ARCHIVIO ISTITUZIONALE
DELLA RICERCA

Alma Mater Studiorum Università di Bologna
Archivio istituzionale della ricerca

VASA-induced cytoplasmic localization of CYTB-positive mitochondrial substance occurs by destructive and nondestructive mitochondrial effusion, respectively, in early and late spermatogenic cells of the Manila clam

This is the submitted version (pre peer-review, preprint) of the following publication:

Published Version:

VASA-induced cytoplasmic localization of CYTB-positive mitochondrial substance occurs by destructive and nondestructive mitochondrial effusion, respectively, in early and late spermatogenic cells of the Manila clam / Reunov A.; Alexandrova Y.; Komkova A.; Reunova Y.; Pimenova E.; Vekhova E.; Milani L. - In: PROTOPLASMA. - ISSN 0033-183X. - STAMPA. - 258:4(2021), pp. 817-825. [10.1007/s00709-020-01601-1]

Availability:

This version is available at: <https://hdl.handle.net/11585/830502> since: 2021-08-27

Published:

DOI: <http://doi.org/10.1007/s00709-020-01601-1>

Terms of use:

Some rights reserved. The terms and conditions for the reuse of this version of the manuscript are specified in the publishing policy. For all terms of use and more information see the publisher's website.

This item was downloaded from IRIS Università di Bologna (<https://cris.unibo.it/>).
When citing, please refer to the published version.

(Article begins on next page)

This is the pre-print version of the following article:

Reunov A, Alexandrova Y, Komkova A, Reunova Y, Pimenova E, Vakhova E, Milani L.
2021 VASA-induced cytoplasmic localization of CYTB-positive mitochondrial
substance occurs by destructive and nondestructive mitochondrial effusion,
respectively, in early and late spermatogenic cells of the Manila clam.
Protoplasma 258. 0033-183X

DOI: 10.1007/s00709-020-01601-1

which has been published in final form at

<https://doi.org/10.1007/s00709-020-01601-1>.

This article may be used for non-commercial purposes in accordance with Springer
Terms and Conditions for Use of Self-Archived Versions.

Protoplasma

VASA-induced cytoplasmic localization of CYTB-positive mitochondrial substance occurs by destructive and non-destructive mitochondrial effusion respectively in early and late spermatogenic cells of the Manila clam

--Manuscript Draft--

Manuscript Number:	PROT-D-20-00300	
Full Title:	VASA-induced cytoplasmic localization of CYTB-positive mitochondrial substance occurs by destructive and non-destructive mitochondrial effusion respectively in early and late spermatogenic cells of the Manila clam	
Article Type:	Original Article	
Corresponding Author:	Arkadiy Reunov Saint Francis Xavier University CANADA	
Corresponding Author Secondary Information:		
Corresponding Author's Institution:	Saint Francis Xavier University	
Corresponding Author's Secondary Institution:	Saint Francis Xavier University	
First Author:	Arkadiy Reunov	
First Author Secondary Information:		
Order of Authors:	Arkadiy Reunov	
	Yana Alexandrova	
	Alina Komkova	
	Yulia Reunova	
	Evgenia Pimenova	
	Evgenia Vakhova	
	Liliana Milani	
Order of Authors Secondary Information:		
Funding Information:	Italian Ministry of Education, University and Research MIUR-SIR Programme (Grant Number RBSI14G0P5) (RBSI14G0P5)	Dr Liliana Milani
Abstract:	<p>To analyze the release of mitochondrial material, a process that is believed to be (i) induced by the VASA protein derived from germplasm granules, and (ii), which appears to play an important role during meiotic differentiation, the localization of the CYTB protein was studied in the process of spermatogenesis of the bivalve mollusc <i>Ruditapes philippinarum</i> (Manila clam). It was found that in early spermatogenic cells, such as spermatogonia and spermatocytes, the CYTB protein shows dispersion in the cytoplasm following the total disaggregation of VASA-invaded mitochondria, what is called here as 'destructive mitochondrial effusion (DME)'. It was found that mitochondria of the maturing sperm cells also uptake VASA. It is accompanied by extramitochondrial transmembrane localization of CYTB assuming mitochondrial content release without mitochondrion demolishing. This phenomenon is called here as 'non-destructive mitochondrial effusion (NDME)'. Thus, in the spermatogenesis of the Manila clam, two patterns of mitochondrial release, DME and NDME, were found, which function, respectively, in early spermatogenic cells and in maturing spermatozoa. Despite the morphological difference, it is assumed that both DME and NDME have a similar functional nature. In both cases, the intramitochondrial localization of VASA coincides with the extramitochondrial localization of the mitochondrial matrix.</p>	

Suggested Reviewers:	<p>Sophie Breton, PhD McGill University s.breton@umontreal.ca Expert in bivalve mitochondria related mechanisms and mollusc gamete formation</p>
	<p>Vladimir Skulachev, Dr.Sci Moscow University skulach@belozersky.msu.ru Expert in the field of mitochondrion destruction in the multicellular animals</p>
	<p>Toshitaka Fujisawa, PhD Department of Developmental Genetics, National Institute of Genetics, Mishima tfujisaw@lab.nig.ac.jp Expert in the study of vasa functions in the metazoan animals</p>
	<p>Mary-Elen Harper, PhD University of Ottawa mharper@uottawa.ca Expert in mitochondrial bionergetics</p>
Opposed Reviewers:	

VASA-induced cytoplasmic localization of CYTB-positive mitochondrial substance occurs by destructive and non-destructive mitochondrial effusion respectively in early and late spermatogenic cells of the Manila clam

Arkadiy Reunov^{1*,2}, Yana Alexandrova², Alina Komkova², Yulia Reunova², Evgenia Pimenova², Evgenia Vekhova², Liliana Milani³

¹St. Francis Xavier University, Department of Biology, Antigonish, NS B2G 2W5, Canada;

²National Scientific Centre of Marine Biology, Far Eastern Branch of Russian Academy of Sciences, Vladivostok, 690041, Russia;

³University of Bologna, Department of Biological, Geological and Environmental Sciences, Via Selmi 3, 40126, Bologna, Italy.

***Author for correspondence:**

Dr. Arkadiy Reunov

St. Francis Xavier University,
Department of Biology,
Antigonish, NS B2G 2W5, Canada;
e-mail: areunov@stfx.ca

Abstract

To analyze the release of mitochondrial material, a process that is believed to be (i) induced by the VASA protein derived from germplasm granules, and (ii), which appears to play an important role during meiotic differentiation, the localization of the CYTB protein was studied in the process of spermatogenesis of the bivalve mollusc *Ruditapes philippinarum* (Manila clam). It was found that in early spermatogenic cells, such as spermatogonia and spermatocytes, the CYTB protein shows dispersion in the cytoplasm following the total disaggregation of VASA-invaded mitochondria, what is called here as ‘destructive mitochondrial effusion (DME)’. It was found that mitochondria of the maturing sperm cells also uptake VASA. It is accompanied by extramitochondrial transmembrane localization of CYTB assuming mitochondrial content release without mitochondrion demolishing. This phenomenon is called here as ‘non-destructive mitochondrial effusion (NDME)’. Thus, in the spermatogenesis of the Manila clam, two patterns of mitochondrial release, DME and NDME, were found, which function, respectively, in early spermatogenic cells and in maturing spermatozoa. Despite the morphological difference, it is assumed that both DME and NDME have a similar functional nature. In both cases, the intramitochondrial localization of VASA coincides with the extramitochondrial localization of the mitochondrial matrix.

Key words Manila clam, spermatogenic cells, mitochondria, VASA, CYTB.

Introduction

Knowledge about the cellular and subcellular characteristics of sperm differentiation in the gonadal niche is important, given the need to develop effective reproductive technologies *in vitro* (Krawetz et al. 2009; Kawasaki et al. 2016; Silva et al. 2018; Sanjo et al. 2018). In the animal kingdom, the development of these approaches is important for targeting restoration of valuable animal species that might be threatened, vulnerable or endangered (Silva et al. 2018).

Bivalve molluscs provide many benefits to society representing a valuable fishing stock having nutritional and pharmacological value (Sakurai et al. 1998; Fernández Robledo et al. 2019; Van der Schatte Olivier et al. 2020). So, a study of bivalve meiotic differentiation is important assuming future development of *in vitro* reproductive approaches for these organisms.

We recently reported data for spermatogenesis of the bivalve mollusc *Ruditapes philippinarum* (Manila clam), that represents the 25% of commercially produced molluscs in the world (Cordero et al. 2017). According to our data, a process that may be decisive for the

differentiation of this mollusc male gametes is the interaction between VASA-positive germ plasm granules (GG) and mitochondria occurring during the transition from mitosis to meiosis. During this event, the VASA protein, spreading in the cytoplasm from disaggregating GG, enters some mitochondria and induces the release of mitochondrial content into the cytoplasm, which is confirmed by the cytoplasmic localization of the mitochondrial protein CYTB (Reunov et al. 2019a). Since the interaction between VASA and mitochondria, as well as the subsequent release of the mitochondrial material, are poorly understood, a more detailed study of these processes appears relevant.

Assuming that the interaction of VASA-positive GG and mitochondria is an important element of the mechanism of sperm differentiation, the modulation of which may play a necessary role in future experiments on sperm differentiation *in vitro*, we investigated the spermatogenesis of the Manila molluscs in more detail. Our special focus was to find out if VASA induced mitochondrial effusion occurs at the late stages of sperm differentiation, and if morphologic traits of this process differs in early and late phases of spermatogenesis.

Materials and Methods

Animal samples

The Manila clam *Ruditapes philippinarum* undergoes an annual reproductive cycle of gametogenesis and spawning that alternates with a period of gonad remodelling. Both testes and ovaries contain a stock of primary mitotic germ cells that are located at the wall of the acini (gonadic units similar to sacks) and periodically enter meiosis followed by gamete formation (Delgado and Perez-Camacho 2007; Milani et al. 2011, 2018). Normally, each acinus contains germ cells at different stage of differentiation, making of *R. philippinarum* a very convenient model species to study gametogenesis machinery.

Confocal microscopy

Portions of mature gonads were collected from adult males and processed according to Milani et al. (2015). In summary, samples were fixed in a solution containing 3.7% paraformaldehyde and 0.1% glutaraldehyde. Samples were rinsed in Phosphate Buffered Saline (PBS) solution and then embedded in agar. Sections of 100–150 µm thickness, obtained using a Lancer Vibratome Series 1000, were post-fixed with increasing concentrations of methanol and rehydrated in Tris Buffered Saline (TBS) solution. After treatment with sodium borohydride in

TBS for a 1 h 30 min at room temperature (RT) and rinsing, antigenic sites were unmasked with 0.01% Pronase E in PBS for 18 min at RT. After washing with PBS, samples were left over night in TBS-1%Triton at 4°C. Next, samples were incubated in 1% Normal Goat Serum (NGS) and 1% BSA in TBS-0.1%Triton (TBS-0.1%T) for 1 h 30 min for blocking non-specific protein-binding sites, then were incubated with anti-VASA (Milani et al. 2015), diluted 1:8,000 in 3% BSA in TBS-0.1%T, leaving 72 h at 4°C. After washing, sections were incubated with 1:400 polyclonal goat anti-rabbit Alexa Fluor 488 (Life Technologies, Carlsbad, USA) in 1% NGS-1% BSA in TBS-0.1%T for 32 h at 4°C. After washing, nuclei were stained with 1 µM TO-PRO-3 nuclear dye (Life Technologies, Carlsbad, USA) in PBS for 10 min at RT and washed. The immunostained sections were mounted in 2.5% 1,4-diazabicyclo[2.2.2] octane (DABCO; Sigma), 50 mM Tris and 90% glycerol. Imaging was performed with a confocal laser scanning microscope (Leica confocal SP2 microscope), using Leica software.

Immunoelectron microscopy

Testes were fixed in 4% paraformaldehyde and 0.5% glutaraldehyde in 0.1 M sodium cacodylate buffer (pH 7.4). After dehydrating the samples through increasing concentrations of ethanol, the pellets were embedded into LR White Resin. The blocks were sectioned with an Ultracut Leica UC6 ultramicrotome (Leica Microsystems, Germany) using a diamond knife. The thin sections were mounted on Formvar-coated nickel grids. The grids were floated on drops of 1% BSA/0.01% Tween 20 in (PBST) for 1 h, then incubated for 1 h with primary antibodies: anti-VASA antibody in rabbit and anti-CYTB antibody in chicken, diluted with PBS-0.05% Tween 20 (PBST) at 1:200 concentration. Next, samples were washed in PBST and incubated for 2 h at RT with a mixture of secondary antibodies diluted 1:50 in PBST. The secondary antibodies used were: 12-nm colloidal gold-conjugated goat anti-rabbit IgG antibody (111-205-144, Jackson) and 18-nm colloidal gold-conjugated goat anti-chicken IgG antibody (703-215-155, Jackson). For control sample preparation, primary antibodies were omitted and only secondary antibodies were used. The grids were washed three times in PBST, rinsed in distilled water, stained with uranyl acetate and lead citrate, and observed and photographed with a Philips 410 Transmission Electron Microscope (Philips Electronics, Eindhoven, The Netherlands).

Transmission electron microscopy

Male gonads were dissected, cut into small pieces, and fixed overnight in primary fixative containing 2.5% glutaraldehyde in 0.1 M cacodylate buffer, pH 7.4, at 4°C. Fixed tissues were

washed in buffer, postfixed in 2% OsO₄ in 0.1 M cacodylate buffer for 2 h, rinsed in 0.1 M cacodylate buffer and distilled water, dehydrated in an ethanol series and acetone, infiltrated and embedded in Spurr's resin. Ultra-thin sections were mounted on slot grids that were coated with formvar film stabilized with carbon. Sections were stained with 2% alcoholic uranyl acetate and aqueous lead citrate and were examined with a transmission electron microscope Zeiss Libra 120 (A Carl Zeiss SMT AG Company, Oberkochen, Germany) and Philips 410 Transmission Electron Microscope (Philips 123 Electronics, Eindhoven, The Netherlands).

Scanning electron microscopy

Gonads were removed, cut into small pieces and fixed for 2–3 h (in 2.5% glutaraldehyde in 0.1M cacodylate buffer, pH 7.4). Primary fixed materials were washed gradually in the same buffer. Washed samples were rinsed in buffer and distilled water, dehydrated in a graded series of ethanol solutions. Sperm suspension was prepared by crushing pieces of fixed materials. The suspension was pipetted onto a Thermanox coverslip (Cat. # 72280) and allowed to settle for 1 h. Coverslips with attached sperm cells were transferred to acetone and critical-point-dried in CO₂. Dried materials were mounted onto aluminum stubs, coated with gold, and examined with a scanning electron microscope LEO-430 (Horus Tech Inc., USA).

Quantitative analysis of mitochondrion dynamics during mitosis-to-meiosis phase

The identification of successive stages of meiotic cells was carried out accordingly to previous descriptions of animal gametogenesis (Reunov et al. 2009; Ables 2015). Spermatogonia (premeiotic cells) have a nucleolus in their dispersed chromatin. Spermatocytes I (cells that entered meiosis) are peculiar in chromatin condensation and in the appearance of distinctive synaptonemal complexes of synapsed chromosomes that occur when chromosomal crossing-over takes place at zygotene-pachytene stage of meiosis.

Three pieces of testis were taken from each of three males, and these pieces were embedded in resin blocks. From each of these nine blocks, three sections were taken from different levels. Thus, 27 sections were investigated. At each section, 10 premeiotic cells and 10 zygotene-pachytene cells were identified, to give a total of 270 cells of each type. Thus, mitochondrial number was calculated in 540 male cells. Mitochondria were identified by electron microscopy and counted. The results were analysed by the Microsoft Excel program. All values are expressed as means with standard error of the mean (SEM). Percentages were calculated using the Student's t-test and $P^* < 0.05$, $P^{**} < 0.001$ were considered statistically significant.

Results

Examination by transmission electron microscopy confirmed our previous data (Reunov et al. 2019a), showing that the cytoplasm of both spermatogonia and primary spermatocytes contains electron-dense germplasm granules (GG) that are round or oval in shape and do not have any surrounding membranes. GG have never been found in contact with mitochondria, but mitochondrial regions that are close to GG usually have an electron-lucent area and swollen membranes (Fig. 1 A). Using immunoelectron microscopy (iEM), we shown that the zygotene-pachytene stage of meiosis is accompanied by a dispersion of GG containing VASA. The GG-derived VASA protein appears to enter neighboring mitochondria (Reunov et al. 2019a). As a result of this study, we found that the penetration of VASA into mitochondria is preceded by the attachment of VASA-positive globules to the mitochondrial surface (Fig. 1 B, C), after which VASA is localized within the mitochondria (Fig. 1 D, E). Using immunoelectron microscopy (iEM) we recorded that VASA appears to induce mitochondrial material release, as supported by cytochrome B (CYTB) localization outside the mitochondria (Reunov et al. 2019a).

To get further evidence of mitochondrial material dispersion process, we used confocal microscopy and showed that spermatogonia, as well as primary spermatocytes, do not only contain CYTB-positive spots that are the size and shape of mitochondria, but their cytoplasm is also stained with antibodies to CYTB (Fig. 2 A, B). Using conventional electron microscopy, we found that the number of mitochondria decreases catastrophically during the transition from mitosis to meiosis, amounting to about 69% in spermatogonia and 31% in primary spermatocytes (Fig. 3 A, B). Early spermatids also have CYTB signals corresponding to the size of mitochondria. However, the cytoplasm of these cells is usually not stained with antibodies to CYTB (Fig. 2 C).

Spermatozoa are the cells having bullet-like nucleus whose apical end is cupped with the acrosome. Mitochondria are located under the basal (wide) end of the nucleus in a collar-like structure called 'midpiece' (Fig. 1 F). These mitochondria surround a centriole that is the basal body of the flagellum growing out from the sperm cell body (Fig. 1 G). The mitochondria are thus assembled in a ring constituted by four organelles and this number is quite constant in the mature spermatozoa (Fig. 1 H).

By confocal microscopy, it was found that the bright CYTB signal is located in the mitochondrial area and could not be found in any other region of spermatozoa (Fig. 2 D). VASA is also regularly found in spermatozoa being located in the mitochondrial area (Fig. 2 E). Large

magnification allows to discriminate the accumulations of faint VASA signal in the midpiece of spermatozoa (Fig. 2 F, G).

iEM analyses showed that VASA presents inside mitochondria (Fig. 1 I). Some VASA signals are found near external mitochondrial membranes and directly on the external membranes (Fig. 1 J). CYTB is seen in the cytoplasm of spermatozoa (Fig. 1 K). In addition, CYTB is found within mitochondria, on mitochondrial external membranes, and outside mitochondria in the immediate vicinity of mitochondrial external membranes (Fig. 1 L).

Discussion

VASA as a possible player in mitochondrial material release

In our previous study using the bivalve mollusc *Ruditapes philippinarum* (Manila clam) as model species, we found that during the mitosis-to-meiosis shift the gradual disappearance of VASA-positive germplasm granules (GG) occurs. The dispersion of GG contributes to VASA dispersion in the cytoplasm that is then followed by VASA localization inside mitochondria (Reunov et al. 2019a). In the course of the present study, we found that during early spermatogenesis, VASA is contained in globules, which represent particles of scattered GG. We found that these VASA-positive globules attach to mitochondria. Thus, although GG have never been found in contact with mitochondria, it can be assumed that VASA is transferred by GG fragments into mitochondria.

We also found that in spermatozoa VASA is localized in the midpiece that contains mitochondria. The origin of VASA in sperms is unclear. In some species, the appearance of VASA in late spermatids and spermatozoa is associated with the dispersion of VASA-positive chromatoid bodies (CB) which arise in spermiogenesis. For example, in the marine medaka *Oryzias melastigma*, whose late spermatids are peculiar in having a CB undergoing dispersion during spermiogenesis, VASA is located inside mitochondria, suggesting intramitochondrial penetration of CB-originated VASA (Reunov et al. 2020). Since, the Manila clam spermatogenic cells have GG but have no CB, VASA presence in sperms may be explained by prolonged presence of the GG originated VASA.

The *vasa* gene has been firstly discovered in *Drosophila* (Lasko and Ashburner 1988; Hay et al. 1990). From then on, VASA homologues have also been found in a number of animal species (see for review Raz 2000; Toyooka et al. 2000; Mochizuki et al. 2001; Sunagara et al. 2006) including humans (Castrillon et al. 2000). This gene encodes an ATP-dependent RNA helicase of the DEAD-box protein family, which plays an important role in many transcriptional

processes, including transcriptional activation (Aratani et al. 2001; Jankowsky 2012). The *vasa* gene is known to show germline-specific expression in many animals and to reside in germ plasm specific structures such as germ plasm granules (Carré et al. 2002). Indeed, the VASA protein is recognized as a main component of germ plasm (Findley et al. 2003). Nonetheless, its germline related function still remains obscure (Gustafson and Wessel 2010). Based on our findings, we believe that during both early and late phases of spermatogenesis of Manila clam VASA plays a role in the release of mitochondrial material.

The forms of mitochondrial effusion differ in early spermatogenesis and spermatozoa

Quantitative analyses showed that during the transition from mitosis to meiosis, there is a noticeable decrease in the number of mitochondria. It seems logic that this event concerns VASA-containing mitochondria that release CYTB-positive mitochondrial substance and undergo elimination. Taking into account that process is accompanied by the complete demolishing of mitochondria, we propose to call this process as ‘destructive mitochondrial effusion’ (Fig. 4 A-C). Given that CYTB did not find in the cytoplasm of spermatids we suggest that destructive mitochondrial effusion does not occur at late stage of sperm formation. Indeed, looking at spermatozoa, we did not record any destruction of mitochondria containing VASA. However, we found that mitochondrial material that is positive for CYTB antibodies locates on the mitochondrial external membranes suggesting the translocation of mitochondrial substance through these membranes. The reasons and mechanisms of the extramitochondrial localization of CYTB-positive substance in spermatozoa remains to be elucidated. It is known that the apoptotic machinery is activated by CYTC modifying mitochondrial membranes to form lipid pores allowing CYTC extramitochondrial leakage (Jangamreddy and Los 2012; Bergstrom et al. 2013). It could not be excluded that mitochondrial efflux in sperms may be accompanied by arising of the membranous pores. Anyway, considering that sperm mitochondrial efflux does not damage the structure of mitochondria, we propose to call this process ‘non-destructive mitochondrial effusion’ (Fig. 4 D-G).

Why does mitochondrial material release occur in spermatogenesis?

The role of mitochondrial material release can be summarized by two current hypotheses: (1) the release of mitochondrial ribosomes may replace cellular ribosomes during early embryogenesis, oogenesis (Kobayashi 1993, 1998; Amikura et al. 2001, 2005) and spermatogenesis (Gur and Breitbart 2006, 2008; Villegas et al. 2002; Reunov et al. 2019b),

or/and (2) the selection of healthy mitochondria occurs along with the elimination of less performing mitochondria (Ghiselli et al. 2019). According to what observed in the early phases of spermatogenesis, the catastrophic process can be theoretically account for hypothesis (2), given the strong reduction in mitochondrial number happening in such stages. However, this hypothesis would need more arguments given that mitochondrial destruction appears to be directly connected to GG and VASA, that were so far not reported as participants in the mitochondrial destruction. The fundamental understanding of mitochondrial destruction was called as ‘mitoptosis’ (Skulachev 2000; Skulachev 2006). Indeed, ‘mitoptosis’ and selective autophagy of mitochondria (‘mitophagy’) are known as specialized processes aimed for elimination of malfunctioning mitochondria (Lyamzaev et al. 2008). Mitophagy provides mitochondrion quality control by removing excessive mitochondrial number or damaged mitochondria (Pickles et al. 2018). In spermatogenesis the mitophagy may be connected with ubiquitination (Nakamura 2013).

It should be emphasized that the release of mitochondrial material that occurs during the mitosis-meiosis phase is morphologically specific in different species of multicellular animals. In some species, the release of mitochondrial substance occurs in a destructive manner. For example, in the spermatogonia of the sea urchin *Anthocidaris crassispina*, mitochondria are grouped using an organizing structure that is formed as a result of the gradual aggregation of two components, which are the GG and the electron-lucent nuage (Fig. 5, 1 A-C). In primary spermatocytes, grouped mitochondria are immersed in the central zone and gradually disappear in the process of dispersion of the entire structural complex (Fig. 5, 1 C-E) (Reunov, 2013). A variant of the destructive process was found in spermatogonia and spermatocytes of the frog *Xenopus laevis*, in which the compact germ granules were found to undergo fragmentation into particles comparable to intermitochondrial cement (IMC) (Fig. 5, 2 A-C). Fragments of the IMC agglutinated some mitochondria of these cells, which led to the formation of mitochondrial clusters (Fig. 5, 2 D, E). The grouped mitochondria lost their membranes, which occurred for the twisting of membrane protrusions around themselves thus forming a multilayer of folded membranes (Fig. 5, 2 E, F). As a result of the twisting of mitochondrial membranes, mitochondrial cores were exposed, which were completely dispersed in the cytoplasm (Fig. 5, 2 G) (Reunov and Reunova, 2016). However, a sample of non-destructive mitochondrial release that does not followed by organelle vanishing, was reported for spermatogenesis of mouse *Mus musculus*. The mitochondria are clustered by fragments of nuage arisen from the GG (Fig. 5, 3 A-C), and only some membranous conglomerates are released from the mitochondria belonging to the cluster although the organelles remain normally shaped (Fig. 5, 3 D, E) (Reunov 2006).

Thus, there are morphological variations in mitochondrial effusion occurring in spermatogenesis of different species, and these differences may have evolutionary reasons that require further study. Considering that the release of mitochondrial material might not always mean the destruction of mitochondria, a kind of functional release of mitochondrial material into the cytoplasm can be assumed. Recently, it was shown that during spermatogenesis of zebrafish, mitochondria, into which VASA entered, released mitochondrial ribosomal subunits, 12S mtrRNA and 16S mtrRNA, into the cytoplasm (Reunov et al. 2019b). This observation obviously adds to the arguments in favor of hypothesis (1). More extended research using *in situ* hybridization and electron microscopy is necessary to verify if cytoplasmic localization of mitochondrial ribosomal subunits is also present in spermatogenic cells of the Manila clam.

Conclusion

In the present study, we documented the possible involvement of the VASA protein in the process of mitochondrial material release (a process having no similarity to mitoptosis), occurring during spermatogenesis of the bivalve mollusc *Ruditapes philippinarum* (Manila clam). Mitochondrial material release is proved by extramitochondrial localisation of the CYTB protein in the cytoplasm. In early spermatogenic cells undergoing a shift from mitosis to meiosis, the release of mitochondrial contents is accompanied by organelle damage and vanishing. In sperms, the release of the CYTB-positive substance occurs without damaging the mitochondria. This is a first microscopy study that (i) shows a possible involvement of VASA in the translocation of mitochondrial material to the cytoplasm of spermatogenic cells, and (ii) shows that mitochondrial effusion occurs by destructive and non-destructive processes that are characteristic for early and late spermatogenic cells, respectively.

Acknowledgements

This study was funded by the Italian Ministry of Education, University and Research MIUR-SIR Programme (Grant Number RBSI14G0P5) funded to LM. We are deeply indebted to Mr. D.F. Fomin (National Scientific Centre of Marine Biology, Far Eastern Branch of Russian Academy of Sciences, Vladivostok, Russia) for helpful assistance during our observations using the electron microscopes. Some part of analyses by electron microscopy were performed in the Microscopy Facility at St. Francis Xavier University (Antigonish, NS, Canada).

Authors' contributions

AR designed the study, implemented most of the TEM work and was a major contributor to writing the manuscript. YA performed material collection/processing and part of the TEM analysis. AK performed part of the TEM analysis. YR performed part of the TEM analysis and the quantitative analysis. EP performed part of the TEM analysis. EV performed the SEM analysis. LM designed the antibody generation, performed material collection/processing, provided images, and was a contributor to discussion and writing the manuscript. All authors read and approved the final manuscript.

Declaration of interest

We declare we have no competing interests.

References

- Ables, E. (2015) *Drosophila* oocytes as a model for understanding meiosis: an educational primer to accompany “Corolla is a novel protein that contributes to the architecture of the synaptonemal complex of *Drosophila*”. *Genetics* 199:17–23
- Amikura R, Kashikawa M, Nakamura, A, Kobayashi S (2001) Presence of mitochondria-type ribosomes outside mitochondria in germ plasm of *Drosophila* embryos. *PNAS* 98:9133-9138
- Amikura R, Sato K, Kobayashi S (2005) Role of mitochondrial ribosome dependent translation in germline formation in *Drosophila* embryos. *Mechanisms of Development* 122:1087-1093
- Aratani S, Fujii R, Oishi T, Fujita H, Amano T, Ohshima T, Hagiwara M, Fukamizy A, Nakajima T (2001) Dual roles of RNA helicase A in CREB-dependent transcription. *Molecular and Cellular Biology* 21:4460-4469
- Bergstrom CL, Beales PA, Lv Y, Vanderlick TK, Groves JT (2013) Cytochrome c causes pore formation in cardiolipin-containing membranes. *PNAS* 110:6269–6274
- Carré D, Djediat C, Sardet C (2002). Formation of a large Vasa-positive germ granule and its inheritance by germ cells in the enigmatic chaetognaths. *Development* 129:661-670
- Castrillon DH, Quade BJ, Wang TY, Quigley C, Crum CP (2000) The human VASA gene is specifically expressed in the germ cell lineage. *PNAS* 97:9585-9590
- Cordero D, Delgado M, Liu B, Ruesink J, Saavedra C (2017) Population genetics of the Manila clam (*Ruditapes philippinarum*) introduced in North America and Europe. *Nature: Scientific Reports* 7, Article number: 39745. 3
- Delgado M, Perez-Camacho A. (2007) Comparative study of gonadal development of *Ruditapes philippinarum* (Adams and Reeve) and *Ruditapes decussatus* (L.) (Mollusca: Bivalvia):

- Influence of temperature. *Scientia Marina* 71:471-484
- Fernández Robledo JA, Yadavalli R, Allam B, Pales-Espinosa E, Gerdol M, Greco S, Stevick RJ, Gómez-Chiarri M, Zhang Y, Heil CA, Tracy AN, Bishop-Bailey D, Metzger MJ (2019) From the raw bar to the bench: Bivalves as models for human health. *Developmental & Comparative Immunology* 92: 260. DOI: 10.1016/j.dci.2018.11.020
- Findley SD, Tamanaha M, Clegg, NJ, Ruohola-Baker H (2003) Maelstrom, a *Drosophila* spindle-class gene, encodes a protein that colocalizes with Vasa and RDE1/AGO1 homolog, Aubergine, in nuage. *Development* 130:859-871
- Ghiselli F, Maurizii MG, Reunov A, Ariño-Bassols H, Cifaldi C, Pecci A, Alexandrova Y, Bettini S, Passamonti M, Franceschini V, Milani L (2019) Natural heteroplasmy and mitochondrial inheritance in bivalve molluscs. *Integrative and Comparative Biology* 59:1016–1032
- Gur Y, Breitbart H (2006) Mammalian sperm translate nuclear-encoded proteins by mitochondrial-type ribosomes. *Genes and Development* 20:411-416
- Gur Y, Breitbart H (2008) Protein synthesis in sperm: Dialog between mitochondria and cytoplasm. *Molecular and Cellular Endocrinology* 282:45-55
- Gustafson EA, Wessel GM (2010) DEAD-box helicases: posttranslational regulation and function. *Biochemical and Biophysical Research Communications* 395:1-6
- Hay B, Jan LY, Jan YN (1990) Localization of vasa, a component of *Drosophila* polar granules, in maternal effect mutants that alter embryonic anteroposterior polarity. *Development* 109:425-433
- Jangamreddy JR, Los MJ (2012) Mitoptosis, a novel mitochondrial death mechanism leading predominantly to activation of autophagy. *Hepat Mon* 12:e6159. doi:10.5812/hepatmon.6159
- Jankowsky E (2011) RNA helicases at work: binding and rearranging. *Trends Biochem Sci* 36:19-29
- Kawasaki T, Siegfried KR, Sakai N (2016) Differentiation of zebrafish spermatogonial stem cells to functional sperm in culture. *Development* 143:566-574
- Kobayashi S, Amikura R, Mukai M (1998) Localization of mitochondrial large ribosomal RNA in germ plasm of *Xenopus embryos*. *Curr Biol* 8:1117-20
- Kobayashi S, Amikura R, Okada M (1993) Presence of mitochondrial large ribosomal RNA outside mitochondria in germ plasm of *Drosophila melanogaster*. *Science* 260:5113-1521
- Krawetz SA, De Rooij DG, Hedger MP (2009) Molecular aspects of male fertility. *International workshop on molecular andrology. EMBO Rep* 10:1087-1092
- Lasko PF, Ashburner M (1988) The product of the *Drosophila* gene *vasa* is very similar to eukaryotic initiation factor-4A. *Nature* 335:611-617

- Lyamzaev KG, Nepryakhina OK, Saprunova VB, Bakeeva LE, Pletjushkina OY, Chernyak BV, Skulachev VP (2008) Novel mechanism of elimination of malfunctioning mitochondria (mitoptosis): Formation of mitoptotic bodies and extrusion of mitochondrial material from the cell. *Biochim Biophys Acta* 1777:817–825. doi: 10.1016/j.bbabi.2008.03.027
- Milani L, Ghiselli F, Maurizii MG, Passamonti M (2011) Doubly uniparental inheritance of mitochondria as a model system for studying germ line Formation. *PLoS ONE* 6(11): e28194. doi: 10.1371/journal.pone.0028194
- Milani L, Ghiselli F, Pecci A, Maurizii MG, Passamonti M (2015) The expression of a novel mitochondrially-encoded gene in gonadic precursors may drive paternal inheritance of mitochondria. *PLoS ONE*, 10(9):e0137468. doi: 10.1371/journal.pone.0137468
- Milani L, Pecci A, Ghiselli F, Passamonti M, Lazzari M, Franceschini V, Maurizii MG (2018) Germ cell line during the seasonal sexual rest of clams: finding niches of cells for gonad renewal. *Histochemistry and Cell Biology*. 148:157–171. doi: 10.1007/s00418-017-1607-z
- Mochizuki K, Nishiyama-Fujisawa C, Fujisawa T (2001) Universal occurrence of the vasa-related genes among metazoans and their germline expression in Hydra. *Dev Genes* 211:299-308
- Nakamura N (2013) Ubiquitination regulates the morphogenesis and function of sperm organelles. *Cells* 2:732-750. doi:10.3390/cells2040732
- Pickles S, Vigié P, Youle RJ (2018). Mitophagy and quality control mechanisms in mitochondrial maintenance. *Curr Biol* 28:170-185. doi:10.1016/j.cub.2018.01.004
- Raz E (2000) The function and regulation of vasa-like genes in germ-cell development. *Genome Biol* 1 (1017):1-6
- Reunov AA (2006) Structures related to the germ plasm in mouse. *Zygote* 14:231-8. doi: 10.1017/S0967199406003789
- Reunov AA (2013) Premeiotic transformation of germ plasm-related structures during the sea urchin spermatogenesis. *Zygote* 21:95-101. doi: 10.1017/S0967199411000402
- Reunov AA, Alexandrova YN, Reunova YA, Komkova AV, Milani L (2019a) Germ plasm provides clues on meiosis: the concerted action of germ plasm granules and mitochondria in gametogenesis of the clam *Ruditapes philippinarum*. *Zygote*. 27:25-35. doi: 10.1017/S0967199418000588
- Reunov AA, Au DW, Alexandrova YN, Chiang MW, Wan MT, Yakovlev KV, Reunova YA, Komkova AV, Cheung NK, Peterson DR, Adrianov AV (2020) Germ plasm-related structures in marine medaka gametogenesis; novel sites of Vasa localization and the unique mechanism of germ plasm granule arising. *Zygote* 28:9-23. DOI: 10.1017/S0967199419000546

- Reunov AA, Reunova YA (2016) Pre-meiotic transformation of germplasm-related structures during male gamete differentiation in *Xenopus laevis*. *Zygote* 24:42-7.
doi: 10.1017/S0967199414000690
- Reunov AA, Yakovlev K, Hu J, Reunova YA, Komkova AV, Alexandrova YN, Pimenova EA, Tiefenbach J, Krause H (2019b) Close association between vasa-positive germ plasm granules and mitochondria correlates with cytoplasmic localization of 12S and 16S mtrRNAs during zebrafish spermatogenesis. *Differentiation* 109:34–41
- Reunov AA, Yurchenko OV, Alexandrova YN, Radashevsky VI (2009) Spermatogenesis in *Boccardiella hamata* (Polychaeta: Spionidae) from the sea of Japan: sperm formation mechanisms as characteristics for future taxonomic revision. *Acta Zoologica* 91:447-456
- Sakurai I, Horii T, Murakami O, Nakao S (1998) Population dynamics and stock size prediction for the sunray surfclam *Macra chinensis* at Tomakomai, southwest Hokkaido, Japan. *Fishery Bulletin* 96:344-351
- Sanjo H, Komeya M, Sato T, Abe T, Katagiri K, Yamanaka H, Ino Y, Arakawa N, Hirano H, Yao T, Asayama Y, Matsuhisa A, Yao M, Ogawa T (2018) *In vitro* mouse spermatogenesis with an organ culture method in chemically defined medium. *PLoS ONE* 13(2):e0192884
- Silva AF, Escada-Rebelo S, Amaral S, Tavares RS, Schlatt S, Ramalho-Santos J, Mota PC (2018) Can we induce spermatogenesis in the domestic cat using an in vitro tissue culture approach? *PLoS One* 13 (2):e0191912
- Skulachev VP (2000) Mitochondria in the programmed death phenomena; a principle of biology: “it is better to die than to be wrong”. *IUBMB Life* 49:365-73
- Skulachev VP (2006) Bioenergetic aspects of apoptosis, necrosis and mitoptosis. *Apoptosis* 11:473-85
- Sunagara T, Saito Y, Kawamura K (2006) Postembryonic epigenesis of Vasa-positive germ cells from aggregated hemoblasts in the colonial ascidian *Botryllus primigenus*. *Develop Growth Differ* 48:87-100
- Toyooka Y, Tsunekawa N, Takahashi Y, Matsui Y, Satoh M, Noce T (2000) Expression and intracellular localization of mouse Vasa-homologue protein during germ cell development. *Mech Dev* 93:139-149
- Van der Schatte Olivier A, Jones L, Le Vay L, Christie M, Wilson J, Malham SK (2020) A global review of the ecosystem services provided by bivalve aquaculture. *Reviews in Aquaculture* 12:3–25
- Villegas J, Araya P, Bustos-Obregon E, Burzio LO (2002) Localization of the 16S mitochondrial rRNA in the nucleus of mammalian spermatogenic cells. *Mol Hum Reprod* 8:977-983

Figure legends

Fig. 1. Spermatogenic cells of the bivalve mollusc *Ruditapes philippinarum* by transmission electron microscopy (TEM), scanning electron microscopy (SEM) and immunoelectron microscopy (iEM).

A, germ plasm granule (GG) in close proximity to the mitochondria (m); note the electron-lucent area and swollen external membranes of mitochondria whose appearance may be induced by GG whose diffused material appears to contact the mitochondrial surface (showed by circle) (TEM).

B, mitochondria and VASA-positive material in the cytoplasm (iEM).

C, an enlarged area squared in Fig. 2 B; note VASA-positive material (two arrowheads) attached to the surface of a mitochondrion (m) (iEM).

D, mitochondria and VASA-positive material (iEM).

E, an enlarged area squared in Fig. 2 D; note VASA-positive material penetrating into a mitochondrion (arrowhead) and also VASA-positive signals (ovals) inside of the mitochondrion (m) (iEM).

F, spermatozoon (SEM); note the spermatozoon substructures, such as acrosome (a), nucleus (n), flagellum (f), and spermatozoon midpiece (in the square) that contains mitochondria (m).

G, spermatozoon (TEM); note the spermatozoon substructures, such as acrosome (a), nucleus (n), flagellum (f), and spermatozoon midpiece (in the square) that contains mitochondria (m).

H, cross section through the spermatozoon midpiece that contains mitochondria; note the four mitochondria (m) arranged in a ring surrounding a centriole (arrows).

I, VASA inside a mitochondrion; magnification of the area squared in black in Fig. 1 H.

J, VASA (showed by circle) on the external membranes (arrows) of a mitochondrion (m).

K, magnification of the area squared in white in Fig. 1 H; note CYTB signals situated in the cytoplasm outside mitochondria (showed by circle).

L, CYTB signals that are present inside a mitochondrion (m), located on the external mitochondrial membranes and outside mitochondrion (showed by oval); arrows show external mitochondrial membranes.

Scale bar = 0.5 μm (A), 0.1 μm (B-E), 1 μm (F, G), 0.5 μm (H), 0.1 μm (I-L).

Fig. 2. Spermatogenic cells of the bivalve mollusc *Ruditapes philippinarum* by confocal microscopy.

A, spermatogonium recognizable by the presence of the nucleolus (nu) in the nucleus (n); note the red CYTB positive cytoplasm (stars) and local CYTB signals corresponding to mitochondria (circles).

B, spermatocyte distinguishable from spermatogonium for the larger areas of condensed chromatin in the nucleus (n); note the red CYTB positive cytoplasm (stars) and more localized CYTB signals corresponding to mitochondria (circles).

C, early spermatid having bright local CYTB red signals that correspond to mitochondria (circles); note that cytoplasm does not show CYTB signal.

D, spermatozoon; note the local red CYTB signal in the spermatozoon midpiece that is situated at the base of the nucleus (n) and corresponds to mitochondrion (circle).

E, spermatozoa having faint red VASA signals in the mitochondrial midpieces.

F, G, magnification of the squared area in Fig. 3 E; note the mitochondrial areas containing faint red VASA signal (circles) in the midpieces of spermatozoa.

Scale bar = 5 μm (A-C), 1 μm (D, F, G).

Fig. 3. Dynamics of the mitochondrial number in spermatogonia (A) and primary spermatocytes (B) of the bivalve mollusc *Ruditapes philippinarum*.

The amount of mitochondria undergo dramatic reduction during mitosis-to-meiosis shift. All values are expressed as means with standard error of the mean (SEM). Percentages were calculated using the Student's t-test and $P^* < 0.05$, $P^{**} < 0.001$ were considered statistically significant.

Fig. 4. Schematic drawings of the destructive (A-C) and non-destructive (D-F) mitochondrial effusion occurring respectively during mitosis-to-meiosis shift and in maturing spermatozoa of the bivalve mollusc *Ruditapes philippinarum*.

Red – VASA, blue dark – CYTB, blue light – mitochondrial content, black lines – mitochondrial membranes. Arrows show direction of mitochondrial release development.

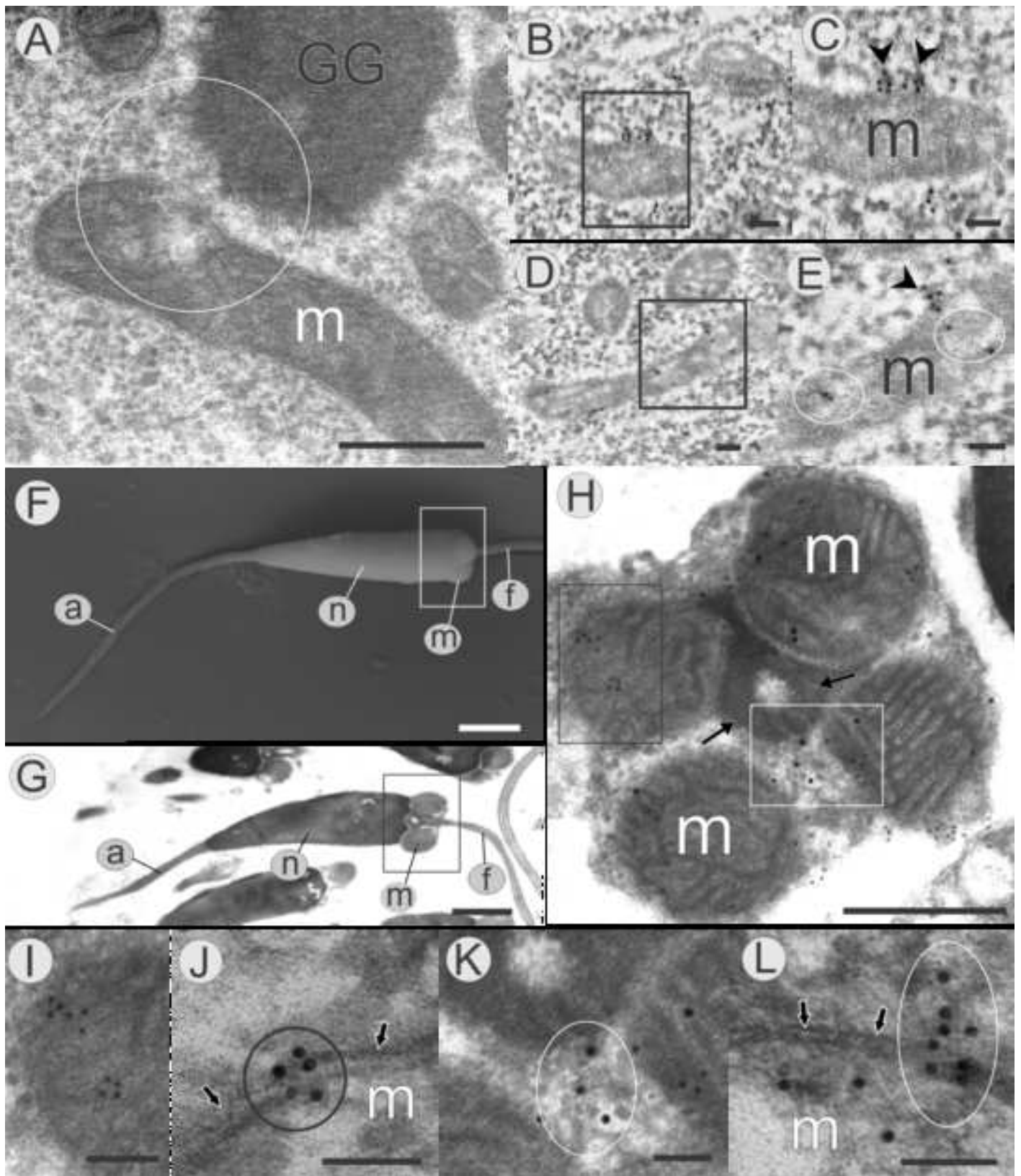
Fig. 5. Schematic drawings of the mitochondrial effusion in the sea urchin *Anthocidaris crassispina* (1), frog *Xenopus laevis* (2), and mouse *Mus musculus* (3). Images were reproduced from [Reunov \(2006; 2013\)](#) and [Reunov and Reunova \(2016\)](#) with permission of Cambridge University Press.

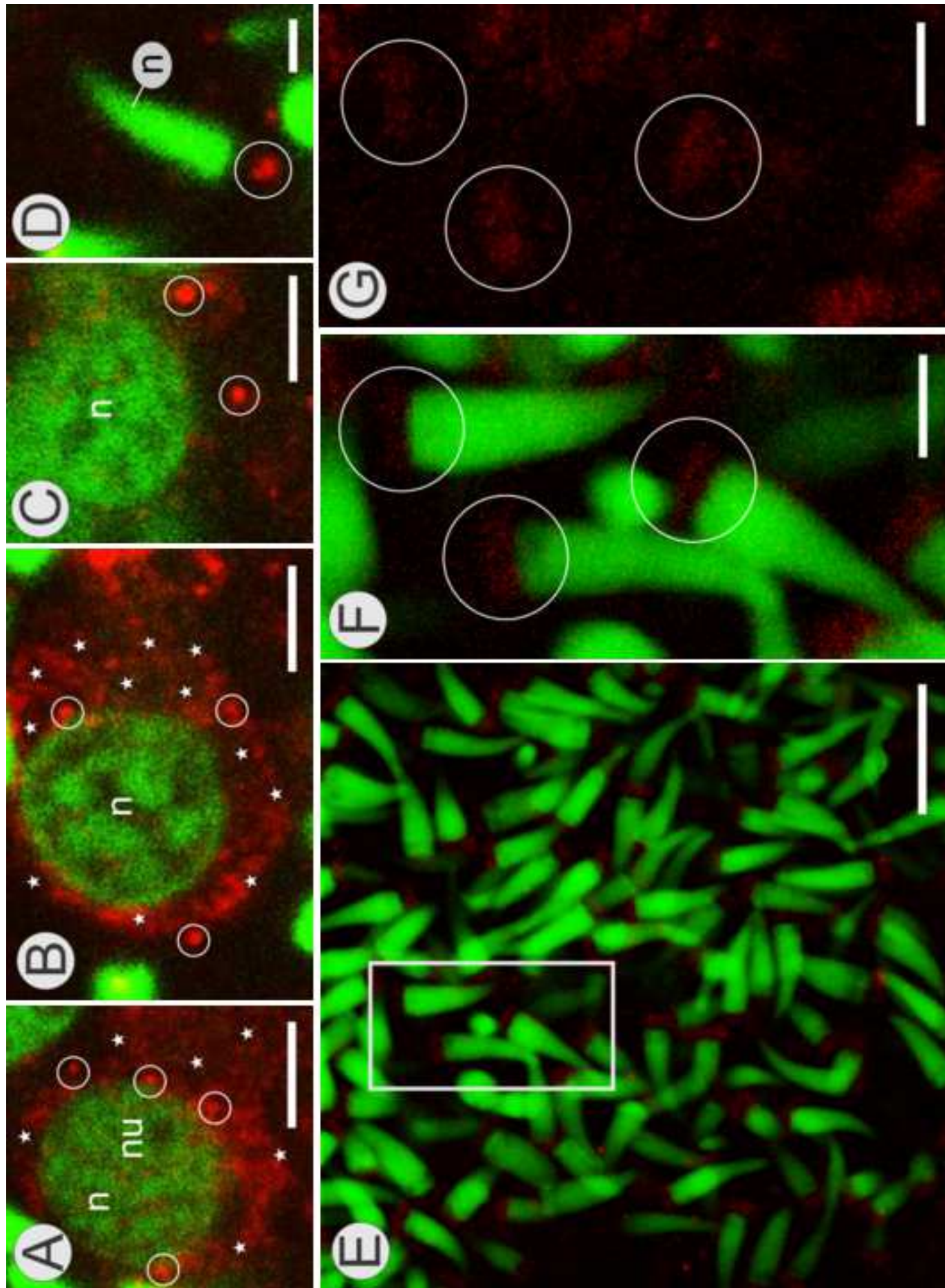
1. Schematic drawings of the germ plasm related structures in the spermatogenic cells of the sea urchin. (A) Germ plasm granule (GG), compact electron-lucent nuage (en) and mitochondria (m). (B) Electron-dense nuage (edn) that arose from germ plasm granules, compact electron-lucent nuage (en) and mitochondria (m) at stage of aggregation. (C) Mitochondrial cluster formed by mitochondria (m) that are aggregated by combined nuage, consisting of electron-dense nuage (edn) and electron-lucent nuage (en); (D) Dispersed nuage (dn) uptaking

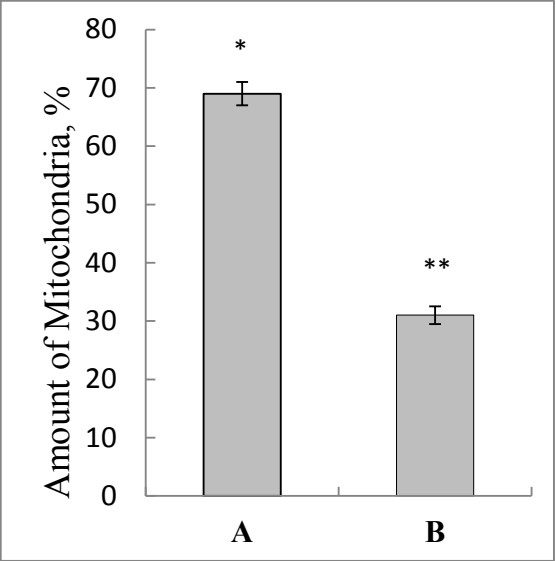
mitochondrial derivatives (md) at dispersion stage. (E) Scattered nuage (sn) at the post-dispersion stage; n, nucleus; s, synaptonemal complexes.

2. Schematic drawings of germ plasm related structures in the spermatogenic cells of the frog. A, compact germ plasm granule (GG); B, C, progressive stages of compact granule dispersion followed by the appearance of relatively smaller fragments; D, E, progressive stages of mitochondrion (m) agglutination by germ plasm granule fragments acting as inter-mitochondrial cement (imc) followed by formation of a mitochondrial cluster; note the appearance of protruded areas (pa) on membranes of clustered mitochondria (E). F, G, formation of multi-layered membranes during progressive twisting of mitochondrial membranes (arrows) followed by formation of naked mitochondrial cores (nmc) which undergo dispersion in the cytoplasm.

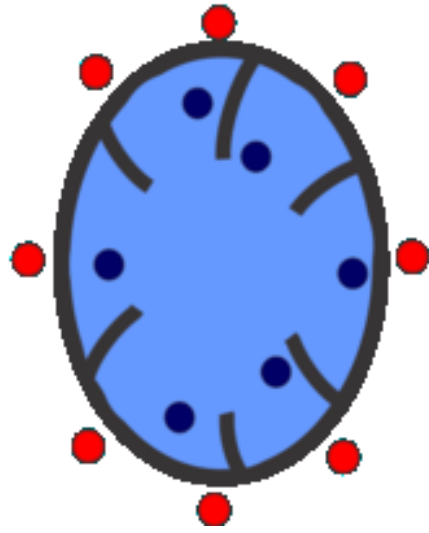
3. Schematic drawings of the germ plasm related structures in the spermatogenic cells of the mouse. (A) Germ plasm granule (GG). (B) Fragmented GG that is called 'nuage' (Ng). (C) Cluster of mitochondria (Mch) aggregated together by nuage fragment (Ngf). (D) Mitochondrial cluster with mitochondria containing membranous conglomerates (Mcg). (E) Mitochondrial cluster with mitochondria excreting membranous conglomerates (Mcg).



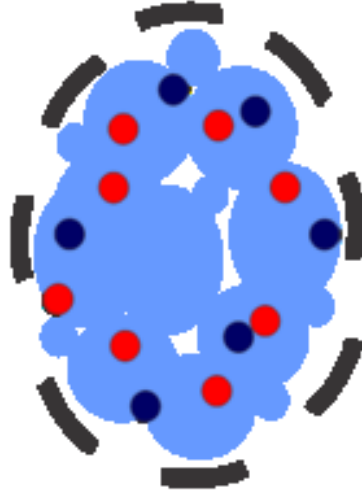




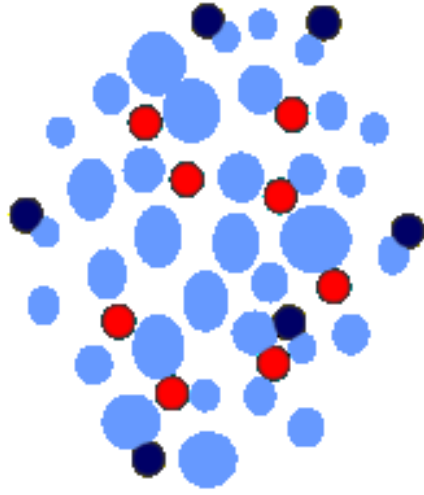
A



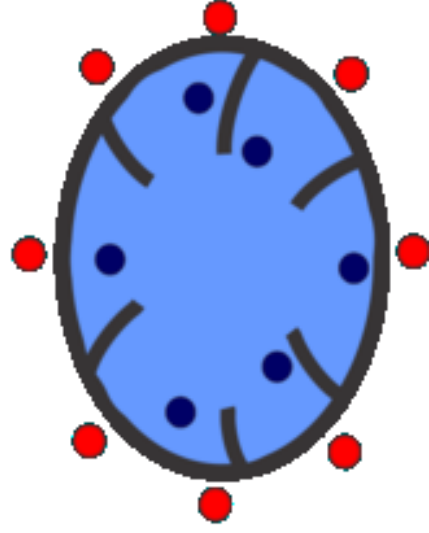
B



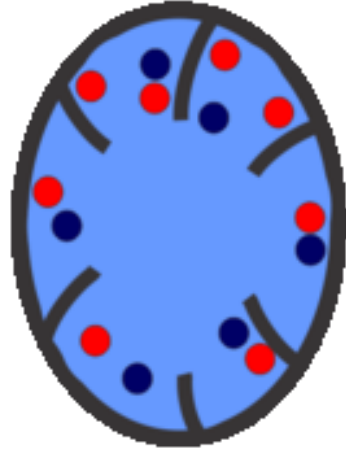
C



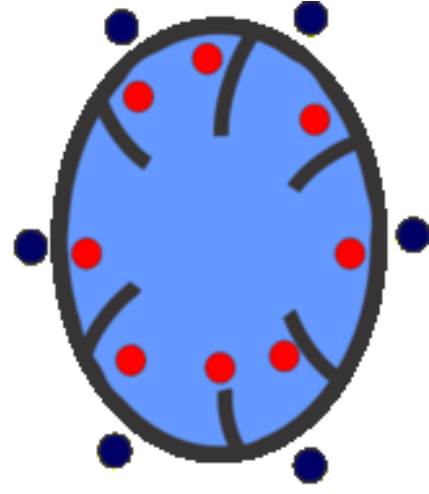
D

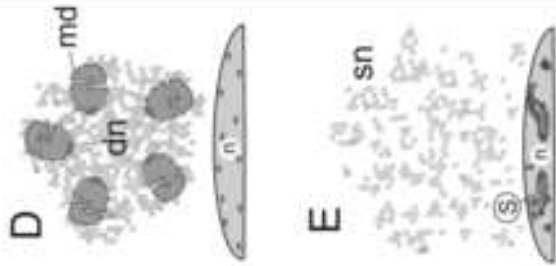
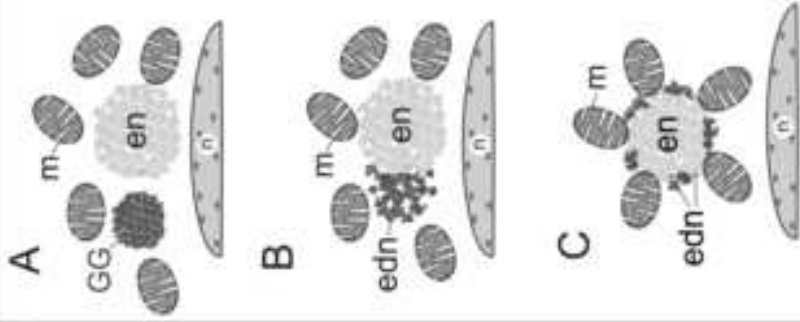
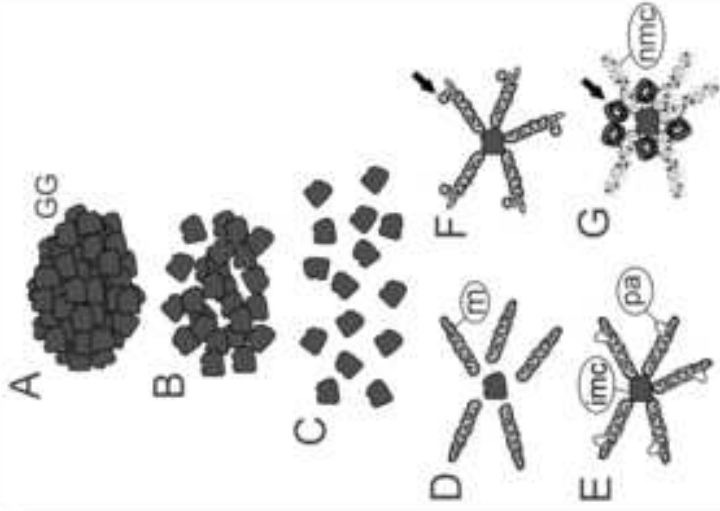
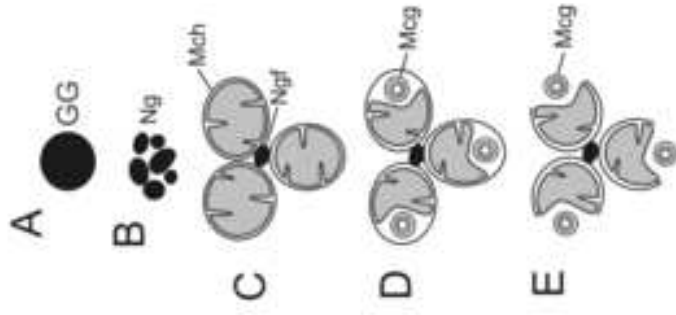


E



F



1**2****3**

1 **Declaration of interest**

2 We declare we have no competing interests.

3